

# INTERACTION BETWEEN LASER BEAM AND ARC IN HYBRID WELDING PROCESSES FOR DISSIMILAR MATERIALS



**C. Thomy**



**F. Möller**



**G. Sepold**



**F. Vollertsen**

**BIAS Bremer Institut für angewandte Strahltechnik, Bremen (Germany)**

## ABSTRACT

Industrial solutions for joining of similar and, most recently, of dissimilar materials are increasingly based on hybrid laser-arc welding processes. To increase the understanding of the synergistic effects of such hybrid processes, it is necessary to investigate the interaction between laser beam and arc. For such investigations, a working head was developed which combines a Nd:YAG laser beam and a plasma arc in a coaxial way. With this equipment the interaction effects between laser and arc were investigated in dependence of laser power, focal position and arc current (AC mode). For process analysis, a high-speed-camera synchronized with a transient recorder (measuring arc current and voltage) was used. In the experimental series reported, an interaction between laser beam and plasma arc resulting in a constriction of weld bead and arc zone and a stabilisation of the foot point of the arc was observed for a wide range of parameter settings. Moreover, for a laser beam intensity exceeding approximately  $6 \cdot 10^5$  W/cm<sup>2</sup> and an AC current below 80 A, the effective arc voltage was significantly reduced. As a working hypothesis, this effect was attributed to the occurrence of laser-induced metal vapour at higher intensities.

**IIW-Thesaurus keywords:** Aluminium; Combined processes; Laser beams; Light metals; Plasma; Radiation; Reference lists.

## 1 INTRODUCTION

Industrial solutions for joining of similar [1-7] and, most recently, of dissimilar materials [8-10] are increasingly based on laser-arc hybrid welding processes such as laser MIG hybrid welding. The general principle in the use of a hybrid laser-arc process for joining dissimilar materials is to create a melt pool in the joining partner with the lower melting temperature and to use the melt to wet the joining partner with the higher melting temperature. This was already successfully demonstrated

for Laser-MIG hybrid joining of aluminium to steel in a variety of application studies based on fundamental research [8, 10]. Figure 1 displays the principle set-up of this process and illustrates some examples for application potentials.

Most recently, a coaxial laser-plasma hybrid welding process was developed by the authors with a special focus on joining aluminium to steel. Although the results achieved so far are quite promising, the optimisation of parameters for such a hybrid welding process still is a challenging task, whether similar or dissimilar materials are considered.

Despite the fact that coaxial or quasi-coaxial arrangements of laser beam and plasma arc have already been considered [11-13], there are only few activities

Doc. IIW-1930-08 (ex-doc IV-961-08) recommended for publication by Commission IV "Power Beam Processes".

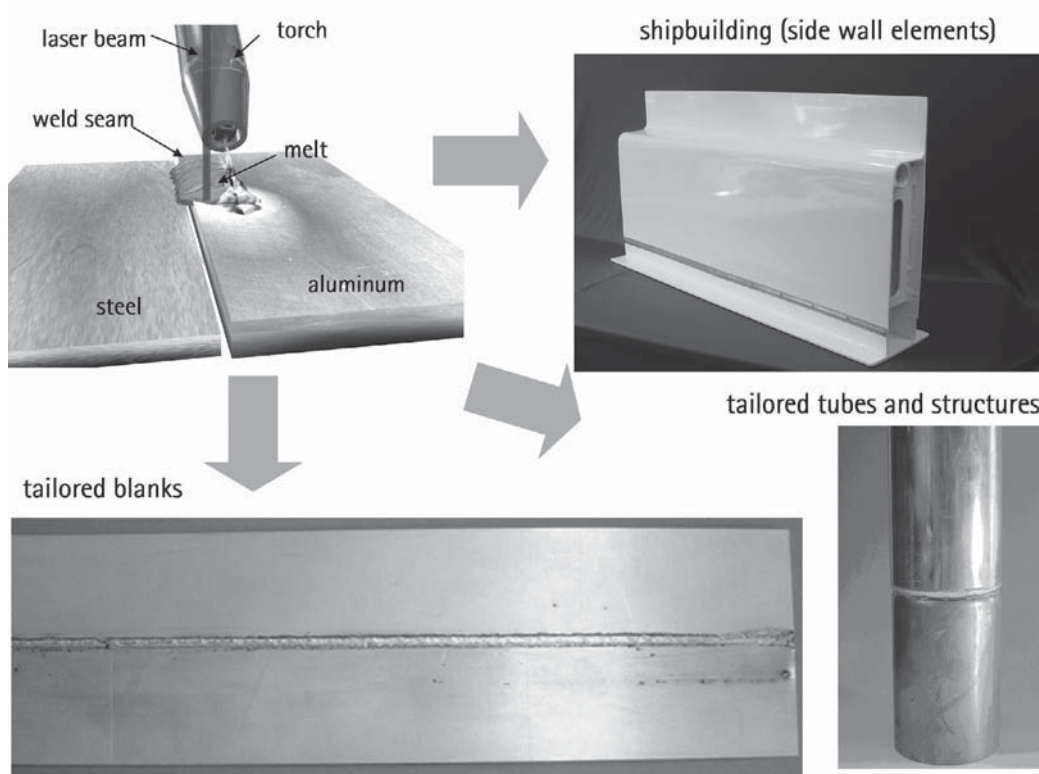


Figure 1 – Process set-up and examples for hybrid welding of aluminium to steel [9, 10]

reported which are related to the fundamental investigation of interaction effects and mechanisms between laser beam and (plasma) arc [14-17]. This is especially true for the case of an AC plasma arc used in hybrid welding. Although it is to be expected that, due to the variety of parameters in such a process, its optimisation would be a challenging task, an AC plasma hybrid welding process would nonetheless be of special interest for aluminium base materials due to the possibility of precisely controlling heat input and cleaning effect.

Therefore, experimental investigations on the interaction between Nd:YAG laser beam and coaxial plasma arc in a practical welding situation would be highly desirable.

## 2 AIM AND SCOPE OF THE INVESTIGATIONS

The investigations reported and discussed in the following were aimed at contributing to an improved understanding of the interaction between laser beam and plasma arc in welding of aluminium in order to lay a basis for an improved exploitation of the advantages of such a hybrid process. To this end, using a specially developed coaxial laser plasma hybrid welding head for bead-on-plate welding on aluminium alloy EN AW-6082, arc current (AC mode), laser power and focal position were varied. In order to identify interaction effects, the welding experiments were performed using process observation (high-speed videography, recording of arc current and voltage).

## 3 EXPERIMENTAL SET-UP, METHODS AND PROGRAMME

### 3.1 Equipment

In this study, a welding head with a specially developed torch directing the laser beam coaxially through a ring-shaped plasma electrode was used (Figure 2). Figure 3 displays the realisation of this principle in a hybrid welding head as well as the set-up for the experimental programme.

The Nd:YAG laser beam (HL 4006D) with a maximum beam power of 4 kW was delivered to the welding head through a fibre with a core diameter of 600  $\mu\text{m}$  and focussed onto the workpiece (beam incidence perpendicular to workpiece) with a set of collimating

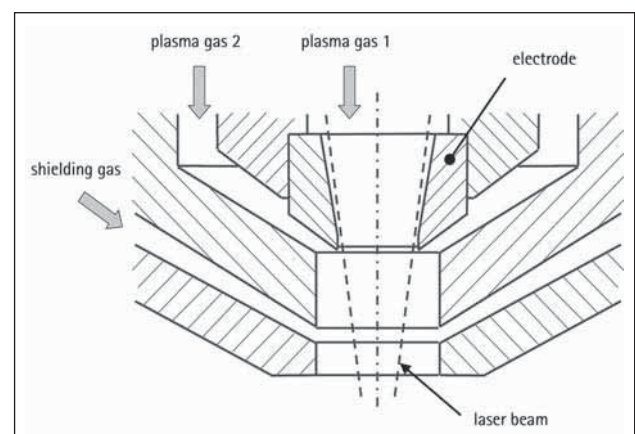
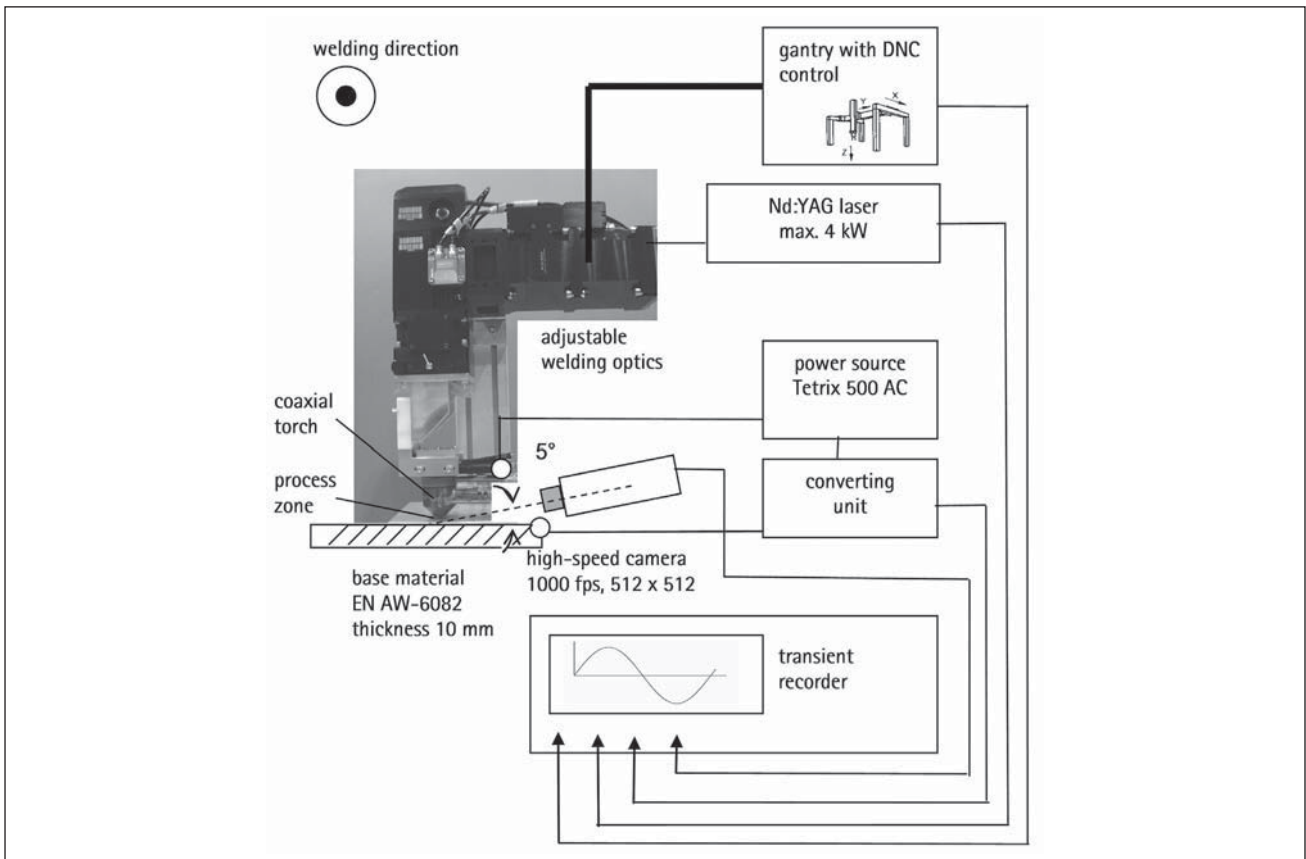


Figure 2 – Principle arrangement for coaxial laser-plasma hybrid welding



**Figure 3 – Coaxial laser-plasma hybrid welding head and experimental setup**

and focussing optics (200 mm each). The collimating optics allowed shifting the focus in positive and negative direction to obtain spot sizes between 0.6 and 3.8 mm at workpiece. The plasma arc power source was a Tetrax 500 AC with a maximum current of up to 500 A, operating in DCEP, DCEN and AC mode. For process observation, a transient recorder recording arc current and voltage (sampled at rate of 25 000 s<sup>-1</sup> via a converting unit connected directly to torch and fixture) was synchronized with a CMOS high-speed-camera (operated at a recording frequency of 1 000 frames per second and a resolution of 512 x 512) and the DNC control of the welding gantry (to obtain start signals for power source, laser and feed). The camera was mounted at an angle of 5° to the horizontal and perpendicular to the welding direction. No additional light source was used.

### 3.2 Experimental programme and procedure

The main parameters and their respective settings varied in the experimental series to investigate interaction effects between laser beam and coaxial plasma arc are given in Table 1.

In special, laser beam power  $P_L$  and spot size  $d$  at workpiece (beam focus within the material) were varied for various settings of arc current  $I_{set}$ . Spot size and laser power were selected to cover a wide range from heat conduction to deep penetration welding. The parameter combination  $P_L = 4$  kW,  $d = 0.6$  mm and  $I_{set} = 70$  A

was applied to 4 welds in order to get an impression on standard deviation for a typical setting.

The most important constant parameters are given in Table 2.

**Table 1 – Parameter variations**

Process parameter			Settings
laser beam power @ workpiece	$P_L$	kW	3.0; 4.0
spot diameter @ workpiece	$d$	mm	0.6; 0.8; 1.2
arc current	$I_{set}$	A	50; 60; 70; 80; 90

**Table 2 – Constant parameters**

Process parameter			Setting
Welding speed	v	m/min	0.5
Type plasma gas 1	---	---	Ar
Flow rate plasma gas 1	---	l/min	0.5
Type plasma gas 2	---	---	Ar
Flow rate plasma gas 2	---	l/min	12
Type shielding gas	---	---	Ar
Flow rate shielding gas	---	l/min	20
Distance nozzle to workpiece	---	mm	6
AC frequency	---	s <sup>-1</sup>	130
Arc balance	---	%	50

All welds were carried out as bead-on-plate welds in EN AW-6082 with a thickness of 10 mm (surface cleaned with alcohol prior to welding). The welding process (welding speed 0.5 m/min) was started as a pure AC plasma welding process at a frequency of 130 Hz. After 10 s, the laser beam was switched on, and the hybrid welding process was continued for 10 s. Thus, by comparing process results and observations, the effect of the laser beam on the arc process could be investigated during one continuous process.

### 3.3 Evaluation methods

The recordings of arc current and voltage were analyzed for effects of the laser beam parameters  $P_L$  and  $d$  on the plasma arc. To this end, signal segments with a duration of 1 s obtained before and after the start of the laser were compared. The segments were extracted 8 s after the start of the arc process and 2 s after the start of the laser. Then, the effective values  $U_{eff}$  and  $I_{eff}$  were calculated as root mean square of the voltage and current signals, respectively. For comparing the signals measured for the pure plasma welding segments ( $P_L = 0$ ) to those measured for the laser plasma hybrid welding segments ( $P_L > 0$ ), the following ratios were calculated, with a ratio of 1 indicating that the laser beam had no effect:

$$\frac{U_{eff}(P_L > 0)}{U_{eff}(P_L = 0)} \cdot \frac{I_{eff}(P_L > 0)}{I_{eff}(P_L = 0)} \quad (1)$$

The high-speed videos were evaluated qualitatively in view of visible laser-arc effects. Moreover, to gain qualitative as well as quantitative information on the size of the arc zone before and after switching on the laser beam, for selected parameter combinations single images were extracted and compared. To this end, 7 single images (statues) covering an AC period of 130 s<sup>-1</sup> were overlaid (to eliminate the effect of arc current and voltage change within one period) and filtered using standard image processing software. For filtering, a so-called solarisation filter was applied, which – in addition to reversing parts of the image in tone – marks areas of contrasting tone (boundary line of arc zone) with a thin line (Figure 4). This method worked well for the boundary lines on the sides of the arc zone. However, the boundary line to the base material was less clearly identified, as reflections of the process light on the aluminium surface in some cases led to artefacts in the filtered image (Figure 4). As these artefacts could always be discerned, they did not impair the use of

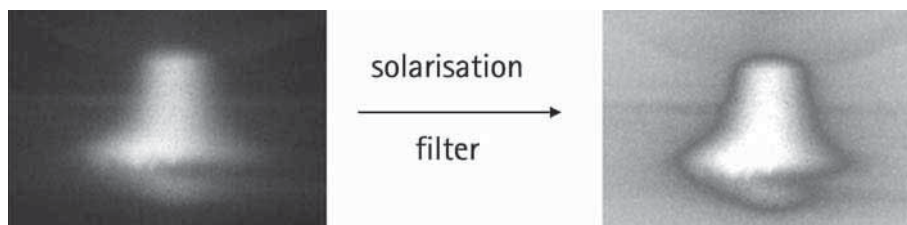


Figure 4 – Example for the processing of overlaid images ( $P_L = 0$  kW,  $I_{set} = 90$  A)

this method for comparing arc size and appearance for various process parameters.

As a basis for correlating results of the process observations with the bead-on-plate welds, all weld surfaces were visually inspected, and cross sections were extracted before and after the position where the laser beam was switched on. These cross sections were then etched and measured (esp. penetration depth  $t$ ).

## 4 RESULTS

### 4.1 General observations

In general, it was observed for most parameter combinations that switching on the laser beam during welding resulted in a decrease in seam width. Whereas the plasma arc without laser beam produced only irregular traces on the aluminium surface (except for  $I_{set} = 90$  A, where some irregular, shallow penetration was observed), switching on the laser resulted in the formation of a weld bead significantly narrower than the arc traces observed without laser beam. A typical example for this effect is given in Figure 5. The observation of the arc for  $P_L = 0$  kW and  $P_L = 3$  kW revealed that, without laser beam, the arc was relatively wide, with its foot point irregularly moving over the sheet surface. In the overlaid images for one AC period, this resulted in a wide arc zone. In contrast, for  $P_L = 3$  kW the arc foot point was more stable, tending to move towards the melt pool generated by the laser process. This was especially obvious for process parameters leading to the formation of a keyhole (small spot size  $d$ ). As a result, the arc zone was significantly constricted.

### 4.2 Effect of laser beam intensity and current $I_{set}$ on penetration depth

As top bead appearance and the high-speed videos had indicated that both laser power  $P_L$  and spot diameter  $d$  can have an influence on the plasma arc stability, the effect of laser beam intensity (calculated as  $P_L / (0.25 \cdot d^2 \cdot \pi)$ ) and current  $I_{set}$  on penetration depth was plotted (Figure 6). For a laser beam intensity at workpiece lower than approx.  $8 \cdot 10^5$  W/cm<sup>2</sup>, penetration remains less than 2 mm, with the cross sections showing the typical characteristics of an arc weld, being 2.8 to 3.9 times wider than deep. Moreover, in most cases the current  $I_{set}$  has a significant effect on penetration depth, with the higher current yielding a higher

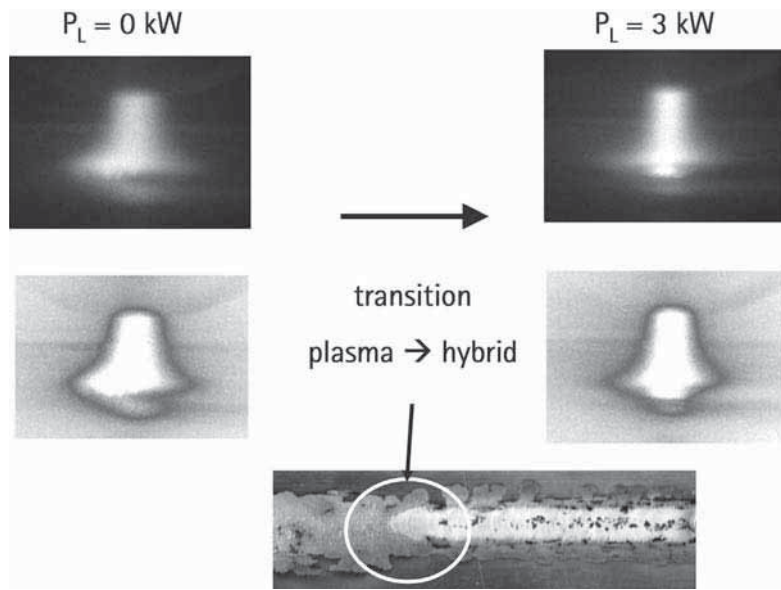


Figure 5 – Example for the effect of laser power on top bead appearance and arc zone geometry (spot size  $d = 0.6 \text{ mm}$ , current  $I_{set} = 50 \text{ A}$ )

penetration. An increase in intensity resulted in a steep, approximately directly proportional rise (correlation coefficient  $R^2 = 0.93$ ) in penetration depth, the width to depth ratio being approximately 1.6 for all parameter combinations. (The regions indicated in Figure 6 will be discussed further in section 5 of this paper.)

### 4.3 Effect of process parameters on arc current and voltage

Figure 7 displays the effect of current  $I_{set}$  and laser beam power  $P_L$  on the effective arc voltage ratio for

$d = 0.6 \text{ mm}$ . Obviously, switching on the laser beam led to a decrease in the effective arc voltage ratio, meaning a decrease in arc voltage for the hybrid process compared to the pure arc process. This decrease is affected by current  $I_{set}$ . Whereas for  $I_{set} < 90 \text{ A}$ , the ratio is generally within the range of 0.9 to 0.95 (taking into account the standard deviation as indicated for  $I_{set} = 70 \text{ A}$ ), for  $I_{set} = 90 \text{ A}$  the effect is less pronounced.

The effective arc current ratio for the same processing conditions is given in Figure 8. A significant effect of the laser beam on the arc current is not observed, as the effective arc current ratio is close to 1.

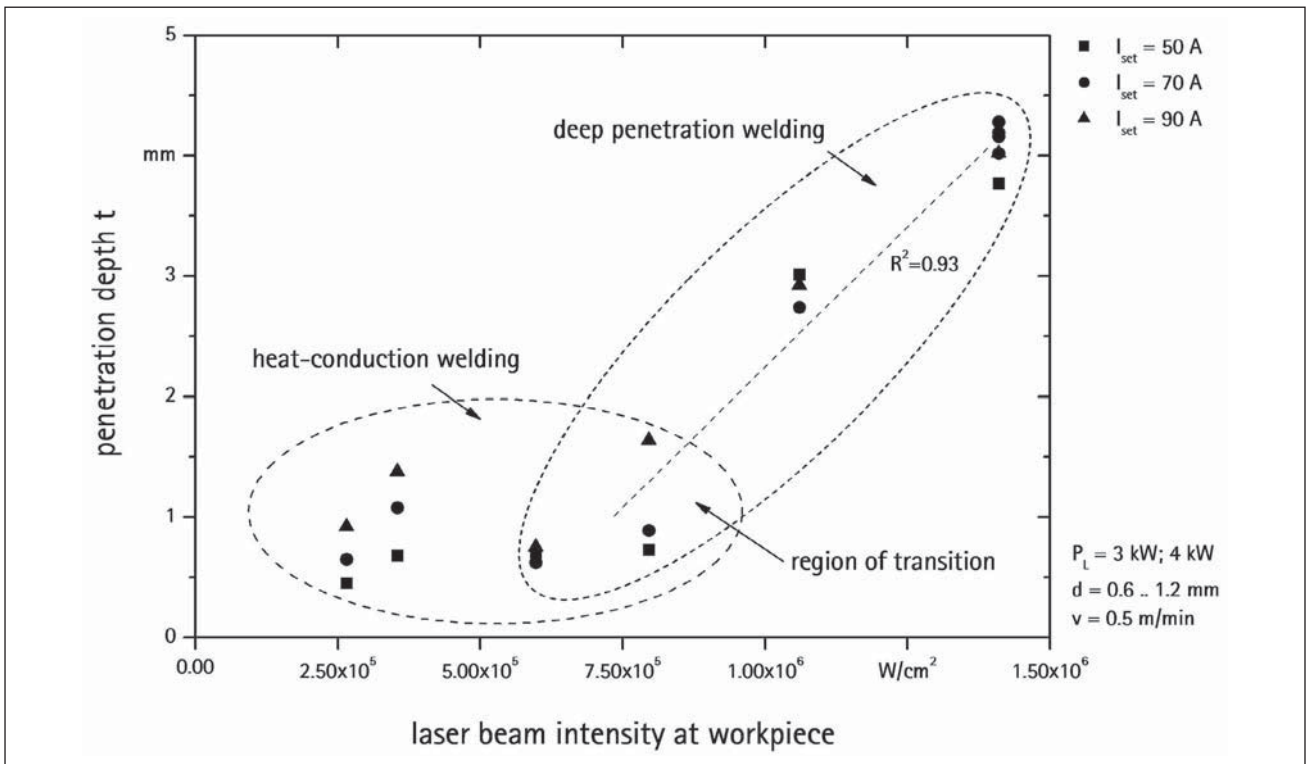


Figure 6 – Effect of laser beam intensity at workpiece and arc current  $I_{set}$  on penetration depth  $t$

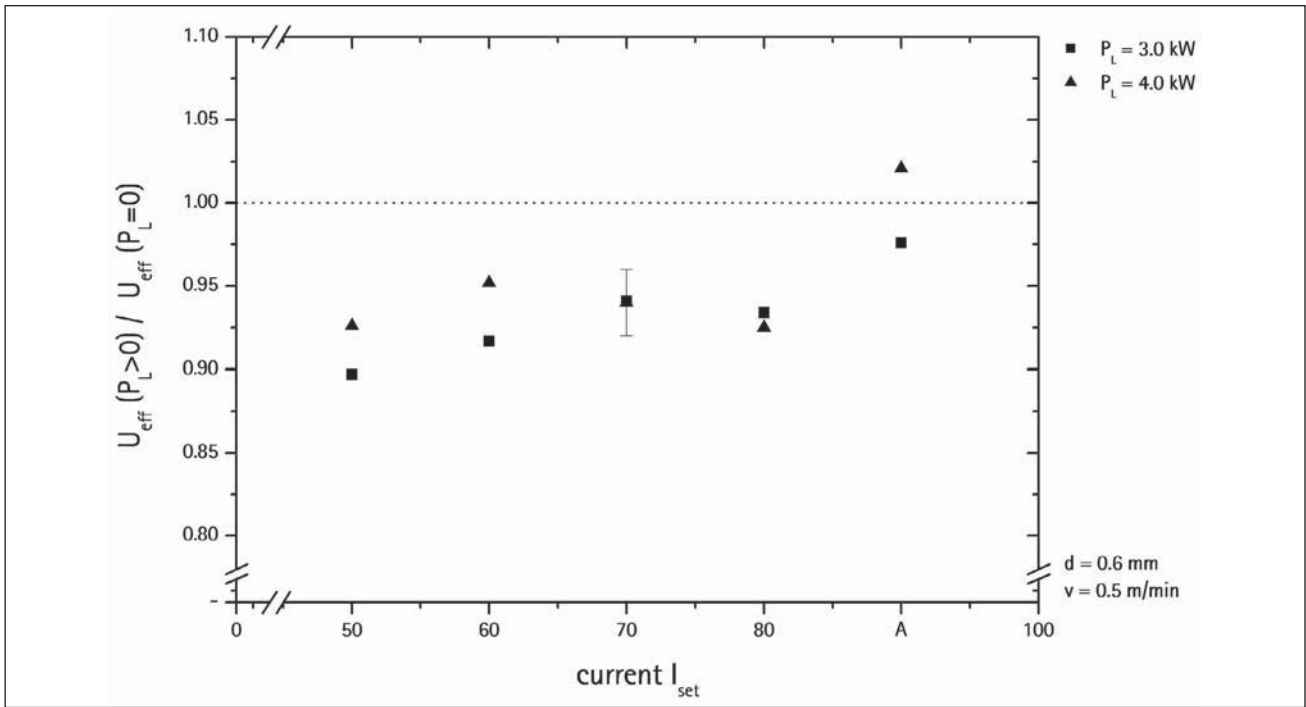


Figure 7 – Effect of current  $I_{set}$  and laser power  $P_L$  on the effective arc voltage ratio

Figure 9 illustrates the effect of current  $I_{set}$  and spot diameter  $d$  on the effective arc voltage ratio for  $P_L = 3$  kW. For  $d = 0.6$  mm and  $0.8$  mm, the arc voltage ratio was significantly and approximately proportionally decreasing with decreasing current  $I_{set}$ . For  $d = 1.2$  mm, the effective arc voltage ratio was slightly above 1, indicating that the laser beam as well as the current  $I_{set}$  did not have a significant effect on the effective arc voltage ratio

As Figures 7 and 9 suggested an influence of laser beam power  $P_L$  and spot diameter  $d$  in dependence of current  $I_{set}$ , the effective arc voltage ratio was plotted

versus laser beam intensity at workpiece (calculated as  $P_L / (0.25 * d^2 * \pi)$ ) for  $I_{set} = 50$  A and  $I_{set} = 90$  A (Figure 10).

For a laser beam intensity at workpiece lower than  $6 * 10^5$  W/cm<sup>2</sup> the effective arc voltage ratio was in the range of 1 for both current settings. At approx.  $6 * 10^5$  W/cm<sup>2</sup>, the effective arc voltage ratio for  $I_{set} = 50$  A was reduced to 0.84 and remained on a comparably low level of approx. 0.9 also for all higher laser beam intensities. For  $I_{set} = 90$  A, the reduction in effective arc voltage ratio was less significant at medium intensities. At higher intensities, the effective arc voltage ratio was again close to 1.

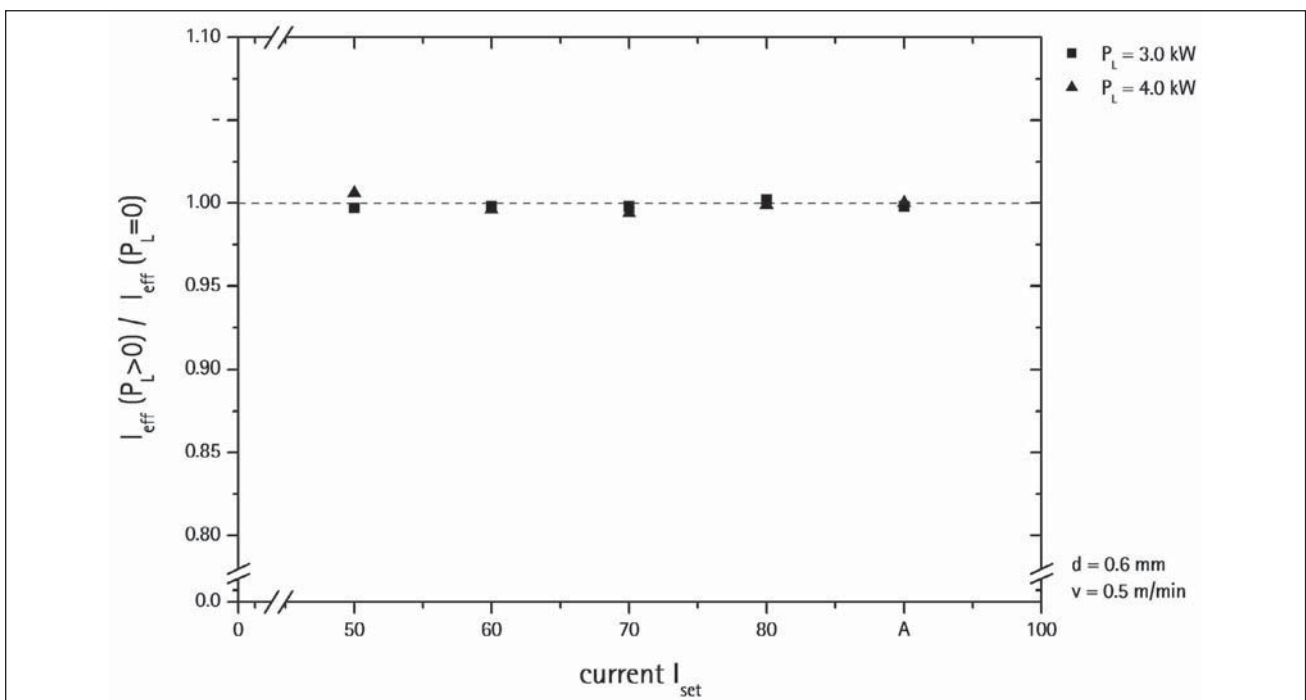


Figure 8 – Effect of current  $I_{set}$  and laser power  $P_L$  on the effective arc current ratio

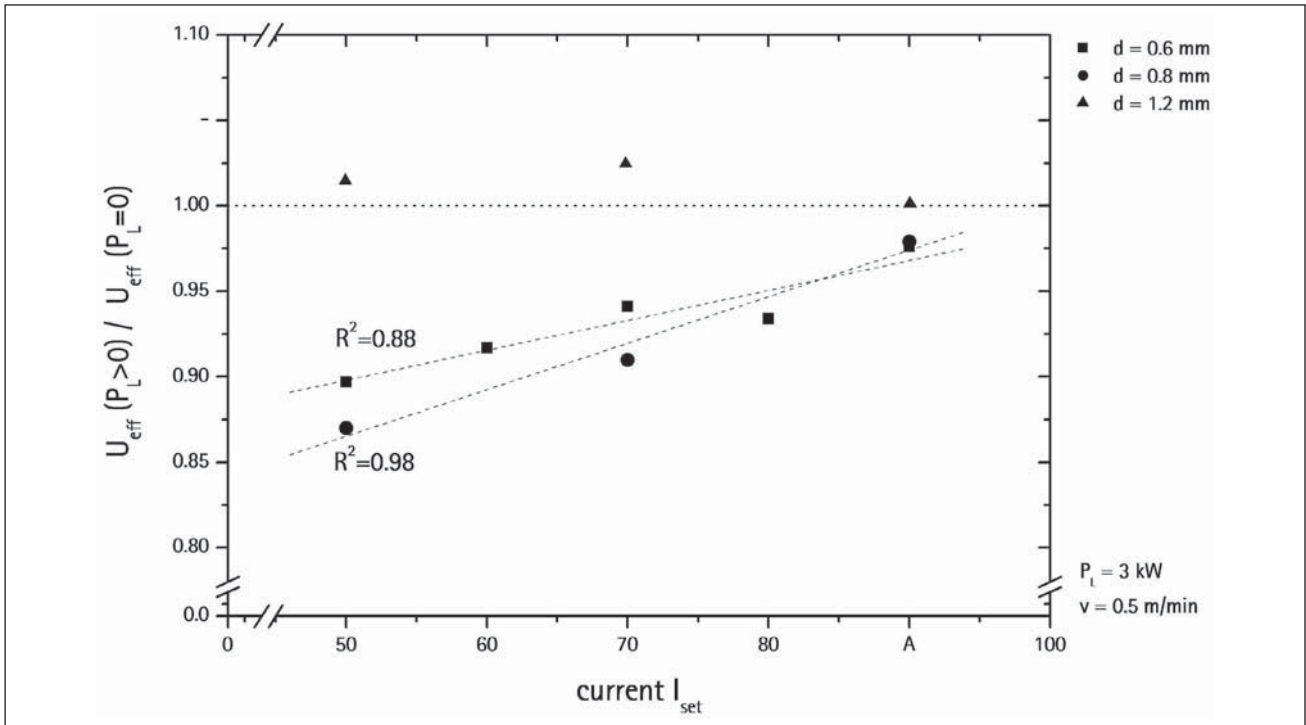


Figure 9 – Effect of current  $I_{set}$  and spot diameter  $d$  on the effective arc voltage ratio

### 5 DISCUSSION

The preliminary results presented above seem to suggest that there indeed is an interaction between Nd:YAG laser beam and plasma arc. This was substantiated not only by qualitative comparison of top bead appearance and high-speed videos (where a constriction of top bead as well as arc zone were observed), but also by the evaluation and comparison of measurements of arc current and voltage.

Whereas effective arc current was not affected by the laser beam, effective arc voltage was for a wide range of parameter settings. The first effect is easily explained by the characteristics of the plasma arc power source, which controls the current to maintain the set waveform. Therefore, only voltage can be affected by any change of processing conditions (provided they remain within a reasonable range). Consequently, the second effect will require a closer look, commenting on the possible nature of the change in processing conditions caused by switching on the laser beam.

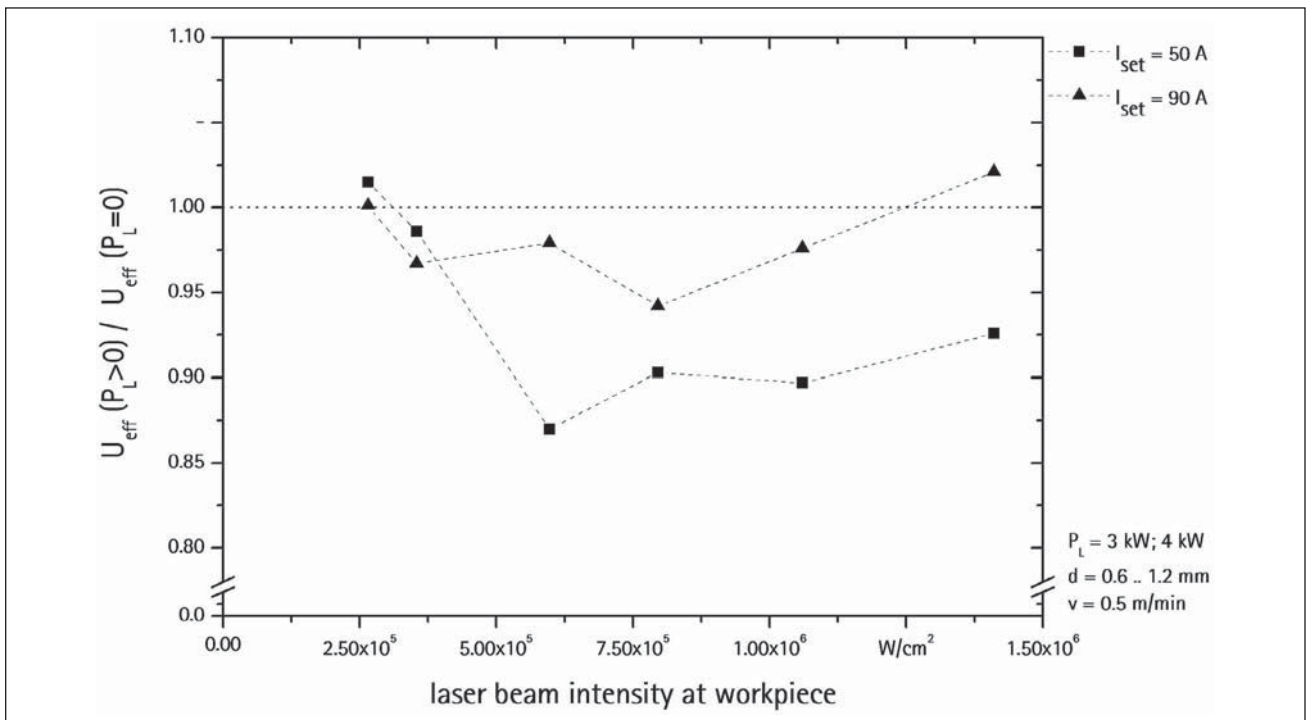


Figure 10 – Effect of laser beam intensity at workpiece and current  $I_{set}$  on the effective arc voltage ratio

Figure 9 gives a significant effect of spot size at workpiece, with a spot size of  $d = 1.2$  mm yielding no influence of the laser beam on the arc at all. As a variation in spot size is equivalent to a variation in laser beam intensity at workpiece, the effective arc voltage ratio was plotted versus laser beam intensity at workpiece for  $I_{set} = 50$  A and  $I_{set} = 90$  A. Again, an effect was found, which was more pronounced for the lower current.

These preliminary results seem to suggest that the change in process conditions affecting arc voltage is related to laser beam intensity at workpiece, which in turn is related to metal evaporation. In the case of deep penetration welding, laser beam intensity at workpiece is sufficient to cause the evaporation of base metal, consequently resulting in the formation of a vapour capillary (keyhole). From this keyhole, a certain amount of metal vapour will be emitted (see e.g. [18]).

For the parameter settings considered within this study, keyhole formation should start in a range between approximately  $6 \cdot 10^5$  W/cm<sup>2</sup> and  $1 \cdot 10^6$  W/cm<sup>2</sup> (see e.g. [18]). For lower intensities, only heat conduction welding should happen. This was substantiated by plotting penetration depth versus laser beam intensity at workpiece (Figure 6), where we positively find deep penetration welding (with a depth-to-width ratio of approx. 1.6) for a laser beam intensity exceeding  $1 \cdot 10^6$  W/cm<sup>2</sup>. For the intensity range between  $6 \cdot 10^5$  W/cm<sup>2</sup> and  $1 \cdot 10^6$  W/cm<sup>2</sup>, the assessment of seam geometry does not allow to positively conclude that a keyhole is formed, as penetration was strongly dominated by arc current, with a higher penetration generally obtained at a higher current. However, process light emissions from the melt pool seem to suggest that a keyhole starts to be formed already at an intensity as low as approx.  $6 \cdot 10^5$  W/cm<sup>2</sup>. An explanation for this may be the pre-heating of the base material by the plasma arc, which reduces the heat input required from the laser beam to reach evaporation temperature. In any case, it should be safe to say a keyhole starts to be formed in the laser beam intensity range between approximately  $6 \cdot 10^5$  W/cm<sup>2</sup> and  $1 \cdot 10^6$  W/cm<sup>2</sup>.

This is exactly the intensity range where the effect of the laser beam started to be detectable both in the high-speed videos and in the effective arc voltage ratio (Figure 10). Therefore, we assume that the formation of a significant additional amount of metal vapour in the process zone over the keyhole is the main factor in the change in process conditions leading to the reduction of the effective arc voltage ratio. As already very small amounts of metal vapour in arc plasma can affect plasma properties by providing a component with lower ionisation energy [e.g. 5.986 eV for Al compared to 15.759 for Ar (see e.g. [19])], electrical conductivity can be greatly influenced (see e.g. [20]). Then, with an increase in electrical conductivity, electrical resistance is decreased, which according to Ohm's law will result in a decrease in voltage for a given current. An indication for a local change in conductivity over the keyhole was also given by the high-speed-videos, which showed that the arc zone was more concentrated over the keyhole (Figure 5). As soon as some amount

of metal vapour was provided (presumably for a laser beam intensity at workpiece exceeding approximately  $6 \cdot 10^5$  W/cm<sup>2</sup>), the effective arc voltage ratio was not significantly affected by a further increase in laser beam intensity (especially for  $I_{set} = 50$  A) (Figure 10).

However, the interaction effect attributed to the occurrence of laser-induced metal vapour tended to be less pronounced for a current  $I_{set}$  exceeding 80 A (Figures 7, 9 and 10). A preliminary explanation approach for this may be found assuming first that the relative amount of laser-induced metal vapour is independent of arc current and second that, with increasing current, the amount of charge carriers in the arc zone is increased. Then, the relative proportion of charge carriers provided by the laser-induced metal vapour should be lower for higher arc current. Consequently, less effect on the effective arc voltage ratio should be expected, which indeed seems to be established within the preliminary experiments presented (esp. Figure 9).

As a conclusion from the preliminary experiments, we assume that a good working hypothesis for further investigating the interaction effects between laser beam and plasma arc would be to assume the main nature of these interaction effects being related to laser-induced metal vapour. Therefore, especially the effects occurring in the transition zone between heat-conduction welding and deep-penetration welding should be studied further.

## 6 CONCLUSIONS

The aim of the investigations reported and discussed within this paper was to contribute preliminary data and hypothesis as a basis for an improved understanding of the interaction between laser beam and plasma arc in welding of aluminium. To this end, using a specially developed coaxial laser plasma hybrid welding head for bead-on-plate welding on aluminium alloy EN AW-6082, arc current (AC mode), laser power and focal position were varied. For identifying interaction effects, the welding experiments were performed using process observation (high-speed video, recording of arc current and voltage).

The experimental results indicated that for a wide range of parameter settings there is indeed an interaction between the laser beam and the arc, resulting in a constriction of weld bead and arc zone and a stabilisation of the foot point of plasma arc. Moreover, effective arc voltage was affected by the laser beam. For a laser beam intensity exceeding approximately  $6 \cdot 10^5$  W/cm<sup>2</sup> and an AC current below 80 A, the effective arc voltage was significantly reduced by the laser beam. As a working hypothesis, this effect was attributed to the occurrence of laser-induced metal vapour at higher intensities.

## ACKNOWLEDGEMENTS

The authors would like to acknowledge the BMBF for funding part of the work presented within the research



project „PROREMIX – Technologiekette zum Produzieren, Reparieren, und Recyclen von Produkten in Material-Mix-Bauweise“ (O2PB2217).

## REFERENCES

- [1] Stauffer H., Rührnöbl M., Miessbacher G.: Hybrid welding for the automotive industry, *Industrial Laser Solutions*, 2003, 10, pp. 7-10.
- [2] Stauffer H., Helten S.: Laser-Hybridschweißen für neuartige Leichtbaukonzepte im Automobilbau (Laser hybrid welding for novel lightweight concepts in automotive engineering). *Proc. Schweißen und Schneiden* 2003, 17. 09. – 19. 09. 2003, Berlin, Germany, pp. 175-180.
- [3] Stauffer A.: Laser hybrid welding and laser brazing at Audi and VW, Document IIW-1610-03 (ex-doc. IV-847-03), *Welding in the World*, 2006, vol. 50, no. 7/8, pp. 44-50.
- [4] Petring D., Fuhrmann C., Wolf N., Poprawe R.: Investigations and applications of laser-arc hybrid welding from thin sheets up to heavy section components, *Proc. 22nd International Congress on Applications of Lasers & Electro-Optics ICALEO*. Chen X., Duley W. (Eds.), 13. 10. – 16. 10. 2003, Jacksonville, FL, USA, pp. 1-10.
- [5] Thomy C., Seefeld T., Vollertsen F.: Laser GMA Hybrid Welding with Various Laser Systems. *Proc. IIW Com. XII Intermediate Meeting*. 16.02. – 18.02. 2005, Wels, Austria, IIW Document XII-1843-05.
- [6] Dahmen M., Bongard K., Kaieler S., Poprawe R., Cottone F.: Hybridschweißen von Öltanks – Ein innovativer Fügeprozeß (Hybrid welding of oil tanks – An innovative joining process), *Technica*, 2001, pp. 46-50.
- [7] Roland F., Lembeck H.: Laser Beam Welding in Shipbuilding – Experience and Perspectives at Meyer Shipyards, *Proc. Lasers in Manufacturing 2001*, June 2001, pp. 463-475.
- [8] Wirth A., Kreimeyer M., Gnauk J., Thomy C., Vollertsen F.: Analyses on the Phase Seam of a Laser-MIG joined Aluminum-Steel Sample, *Proc. 4th International WLT-Conference on Lasers in Manufacturing LIM 2007*, Vollertsen F.E.A. (Ed.), June 18-22, 2007, Munich, Germany, pp. 111-115.
- [9] Thomy C., Wirth A., Kreimeyer M., Wagner F., Vollertsen F.: Joining of Dissimilar Materials – New Perspectives for Lightweight Design in the Transportation Industrie, In *Proc. IIW International Conference Welding & Materials*, July 01-08, 2007, Dubrovnik & Cavtat, Croatia, pp. 311-326.
- [10] Thomy C., Wagner F., Vollertsen F., Metschkow B.: Lasers in the Shipyards – Laser Joining of Aluminum to Steel for Modern Yacht Construction, *Industrial Laser Solutions*, 2007, 11, pp. 9-13.
- [11] Fuerschbach P.: Laser Assisted Plasma Arc Welding, In *Proc. International Conference on Laser Applications and Electro Optics ICALEO*, Denney P., Miyamoto I., Watkins K. (Eds.), 1999, pp. 102-109.
- [12] Ishide T., Tsubota S., Watanabe M.: Latest MIG, TIG Arc – YAG Laser Hybrid Welding Systems for Various Welding Products, In *Proc. First International Symposium on High-Power Laser Macroprocessing*, 27-31.05 2003, pp. 347-352.
- [13] Petring D.: Hybrid Laser Welding. *Industrial Laser Solutions*, 2001, 12, pp. 12-16.
- [14] Cui H.: Untersuchung der Wechselwirkungen zwischen Schweißlichtbogen und fokussiertem Laserstrahl und der Anwendungsmöglichkeiten kombinierter Laser-Lichtbogentechnik (Investigation of the interactions between welding arc and focused laser beam and application potentials of a combined laser-arc technique), *Dissertation*, TU Braunschweig, Fakultät für Maschinenbau und Elektrotechnik, 1991.
- [15] Gvozdetzky V., Krivtsun I., Chizhenko M., Yarinich L.: *Laser-Arc Discharge: Theory and Applications*. Harwood Academic Publishers, 1995.
- [16] Seyffarth P., Krivtsun I.: *Laser-Arc Processes and their Applications in Welding and Material Treatment*, Taylor & Francis, 2002.
- [17] Aden M., Kreutz E., Hausen O., Poprawe R.: Influence of the laser radiation on the plasma dynamics during arc-laser welding, In *Proc. International Congress on Applications of Lasers and Electro Optics (ICALEO)*, 1998, Orlando, FL, USA.
- [18] Beyer E.: *Schweißen mit Laser (Welding with laser)*, Springer Verlag, 1995.
- [19] N.N.: Tabellen zur Quantenphysik, In *Taschenbuch der Physik (Tables on quantum physics, In: Handbook of physics)*, Stöcker H. (Ed.), Harri Deutsch, 2000, 989ff.
- [20] Schellhase M.: *Der Schweißlichtbogen – ein technologisches Werkzeug (The welding arc – a technological instrument)*, DVS-Verlag, 1985.